

Electronic Supplementary Information (ESI)

Unusual anion effect on the direction of three-dimensional (3-D) channel-like silver(I) coordination frameworks with isonicotinic acid N-oxide

Miao Du,* Cheng-Peng Li and Jian-Hua Guo

College of Chemistry and Life Science, Tianjin Key Laboratory of Structure and Performance for Functional Molecule, Tianjin Normal University, Tianjin 300387, P. R. China

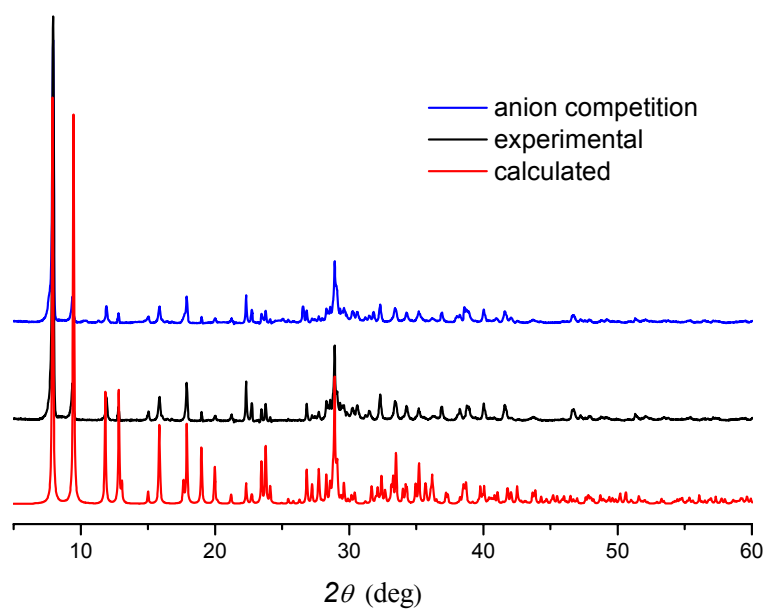
* Corresponding author. E-mail: dumiao@public.tpt.tj.cn

Experimental

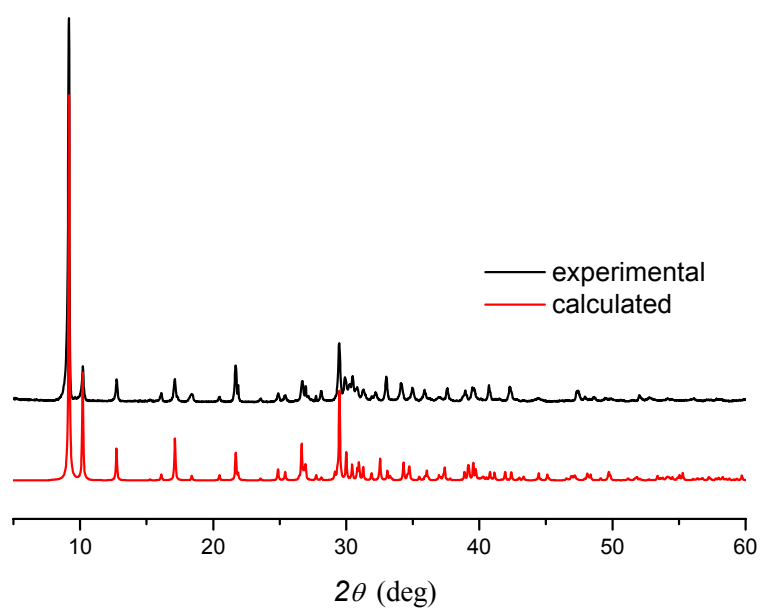
Materials and general methods. All starting materials and solvents were commercially available and used as received. Fourier transform (FT)-IR spectra (KBr pellets) were recorded on an AVATAR-370 (Nicolet) spectrometer. The absorption bands are denoted as follows: broad – b, medium – m, (very) strong – (v)s, and weak – w. Elemental analyses of C, H, and N were performed by using a CE-440 (Leemanlabs) analyzer. Thermogravimetric analysis (TGA) experiments were carried out on a NETZSCH TG209 (Siemens) thermal analyzer from 25 to 800 °C under nitrogen atmosphere at a heating rate of 10 °C/min. Powder X-ray diffraction (PXRD) patterns were taken on a Rigaku D/max-2500 diffractometer for Cu K α radiation ($\lambda = 1.5406 \text{ \AA}$), with a scan speed of 2 °/min and a step size of 0.02° in 2θ . The calculated PXRD patterns were obtained from single-crystal X-ray diffraction data.

Single-crystal X-ray diffraction. X-ray diffraction data were collected on a Bruker Apex II CCD diffractometer with Mo K α radiation ($\lambda = 0.71073 \text{ \AA}$) at room temperature.

In each case, a semi-empirical absorption correction was applied using SADABS and the SAINT program was used for integration of the diffraction profiles (Bruker AXS, *SAINTE Software Reference Manual*, Madison, 1998). The structure was solved by direct methods using SHELXS program of SHELXTL package and refined with SHELXL (G. M. Sheldrick, *SHELXTL NT Version 5.1. Program for Solution and Refinement of Crystal Structures*, University of Göttingen, Germany, 1997). The final structural refinement was carried out by full-matrix least-squares methods on F^2 with anisotropic thermal parameters for all non-H atoms. Generally, C-bound hydrogen atoms were located geometrically and refined as riding, whereas O-bound ones (carboxyl for **1** and water for **2**) were first determined in difference Fourier syntheses and then fixed at the calculated positions. Isotropic displacement parameters of the hydrogen atoms were derived from their parents. The perchlorate counter anion in **1** was treated by using a disorder model with the occupancy ratio of 0.5.

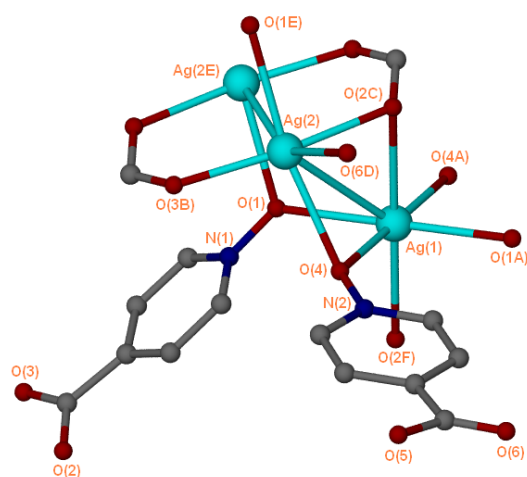


(a)

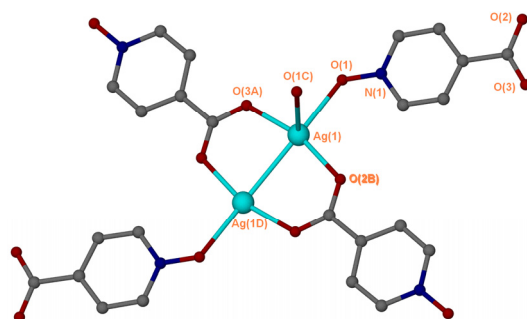


(b)

Fig. S1 Powder X-ray diffraction (PXRD) patterns of (a) **1** and (b) **2**.



(a)



(b)

Fig. S2 Local coordination environments of Ag^I in (a) **1** and (b) **2**. Symmetry codes for **1**: A = $-x, -y + 2, -z + 2$; B = $-x + 1, -y + 1, -z + 2$; C = $x, y + 1, z$; D = $-x, -y + 2, -z + 1$; E = $-x + 1, -y + 2, -z + 2$; F = $-x, -y + 1, -z + 2$; for **2**: A = $-x + 2, y - 1/2, -z + 3/2$; B = $x + 1, -y + 3/2, z - 1/2$; C = $x + 1, y, z$; D = $-x + 3, -y + 1, -z + 1$.

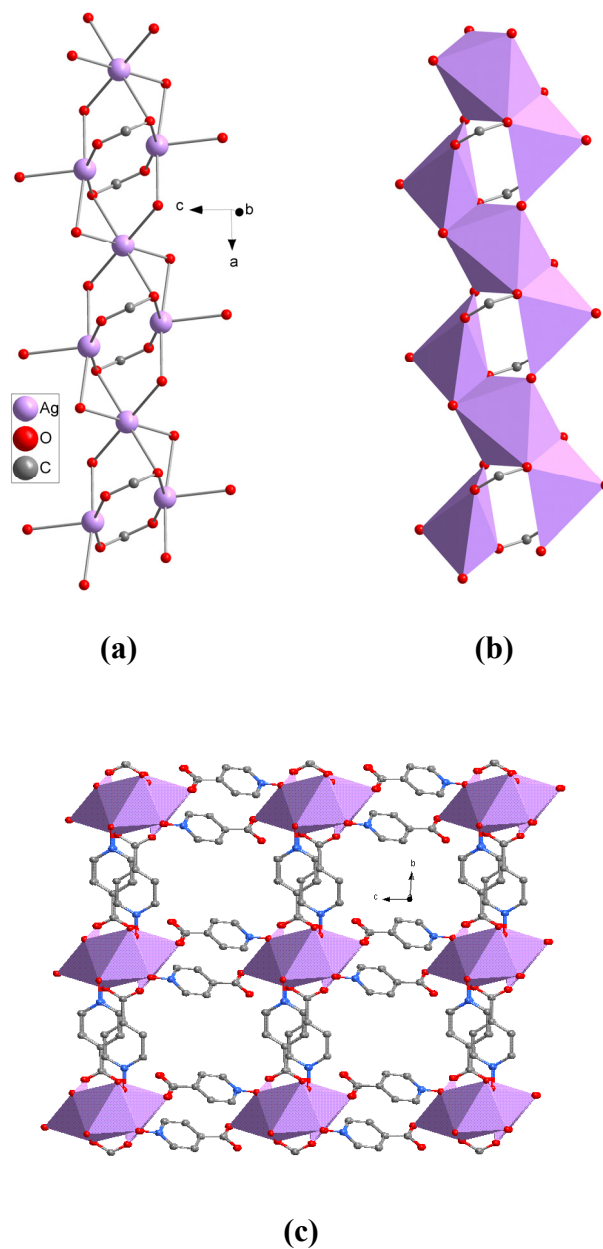
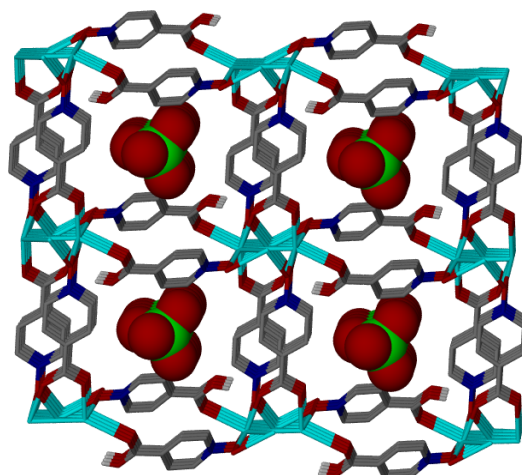
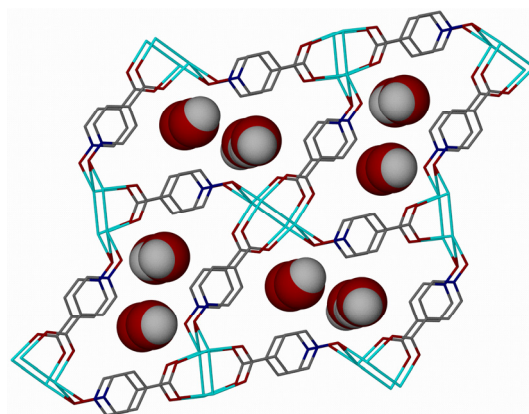


Fig. S3 Views of complex **1**. (a) Ball and stick representation of the 1-D Ag–O–C array. (b) 1-D Ag–O–C rod with Ag^I centers shown as polyhedra. (c) 3-D coordination framework extended by the linkage of 1-D Ag–O–C rods via ligand backbones.



(a)



(b)

Fig. S4 3-D network structures of (a) **1** and (b) **2** (the included anions in **1** and water molecules in **2** are represented by using the space-filling model).

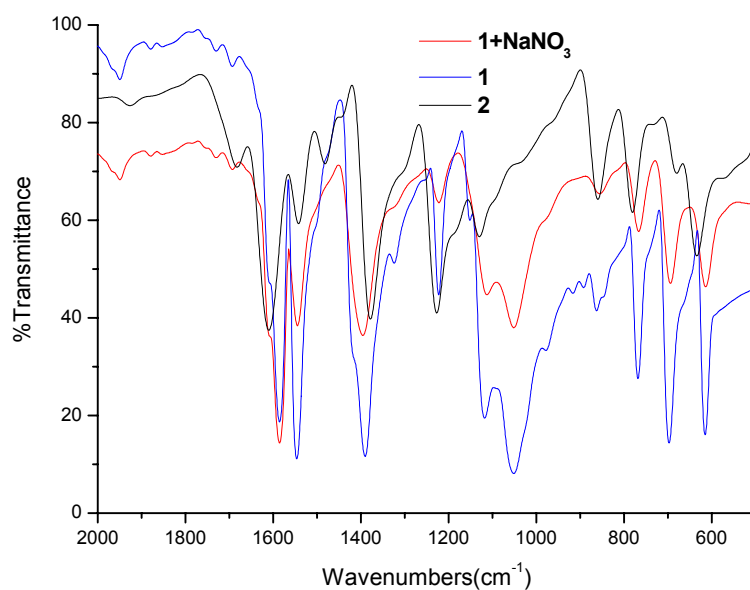


Fig. S5 IR spectra for **1**, **2**, and the anion exchange product **1a** (**1** + NaNO₃). Elemental analysis for **1a**: C, 29.61; H, 1.97; N, 5.63%. Anal. Calcd for **1**: C, 29.49; H, 1.86; N, 5.73%; for **2**: C, 27.30; H, 2.29; N, 5.31%.

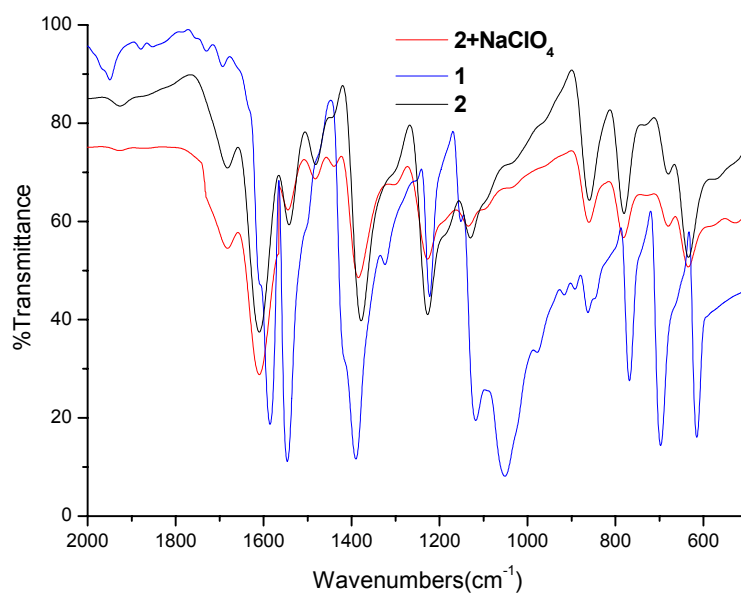


Fig. S6 IR spectra for **1**, **2**, and the guest exchange product **2a** (**2** + NaClO₄). Elemental analysis for **2a**: C, 27.11; H, 2.36; N, 5.43%. Anal. Calcd for **1**: C, 29.49; H, 1.86; N, 5.73%; for **2**: C, 27.30; H, 2.29; N, 5.31%.

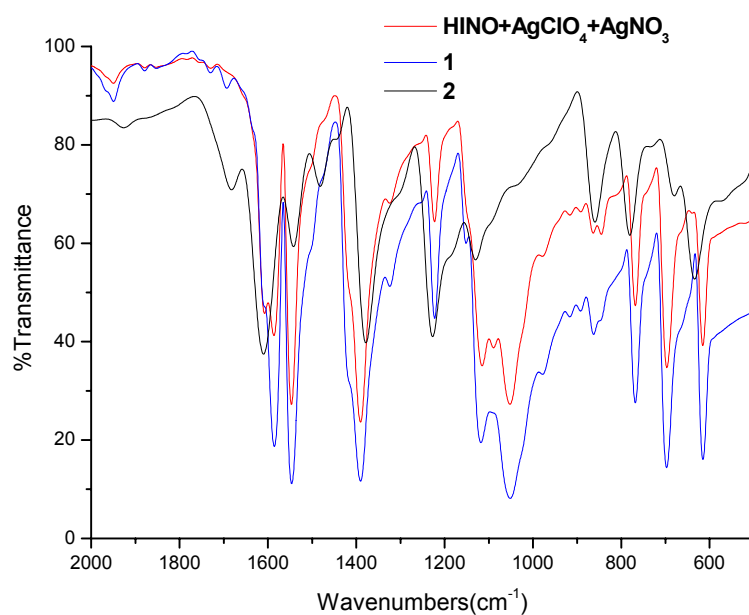


Fig. S7 IR spectra for **1**, **2**, and the anion competition product **1b** (HINO + AgClO₄ + AgNO₃). Elemental analysis for **1b**: C, 29.66; H, 1.65; N, 5.67%. Anal. Calcd for **1**: C, 29.49; H, 1.86; N, 5.73%; for **2**: C, 27.30; H, 2.29; N, 5.31%.

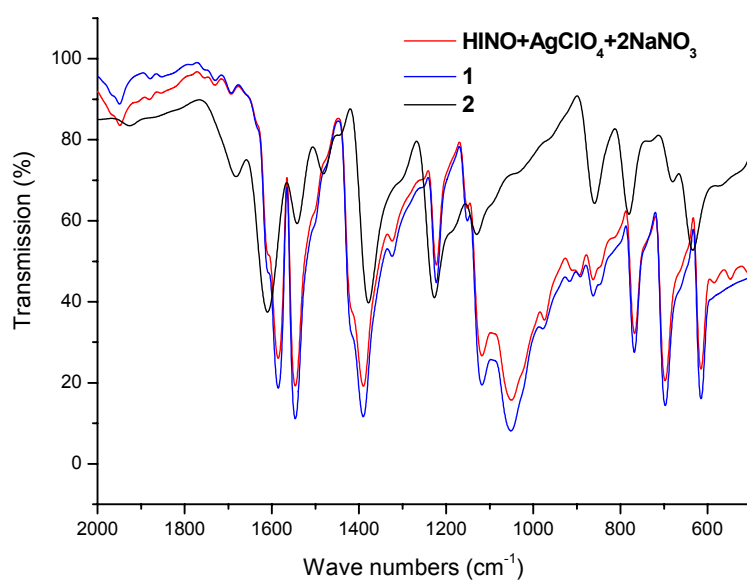


Fig. S8 IR spectra for **1**, **2**, and the anion competition product **1c** (HINO + AgClO₄ + 2NaNO₃). Elemental analysis for **1c**: C, 29.38; H, 1.64; N, 5.42%. Anal. Calcd for **1**: C, 29.49; H, 1.86; N, 5.73%; for **2**: C, 27.30; H, 2.29; N, 5.31%.

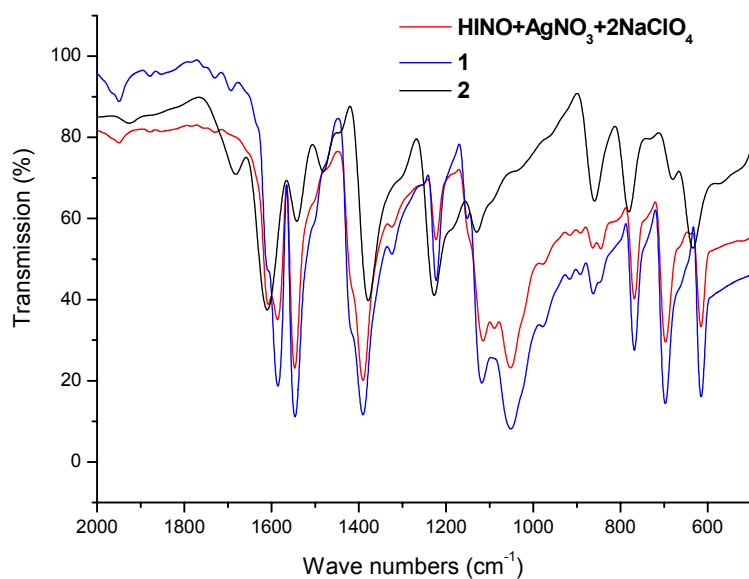


Fig. S9 IR spectra for **1**, **2**, and the anion competition product **1d** (HINO + AgNO₃ + 2NaClO₄). Elemental analysis for **1d**: C, 29.69; H, 1.71; N, 5.82%. Anal. Calcd for **1**: C, 29.49; H, 1.86; N, 5.73%; for **2**: C, 27.30; H, 2.29; N, 5.31%.

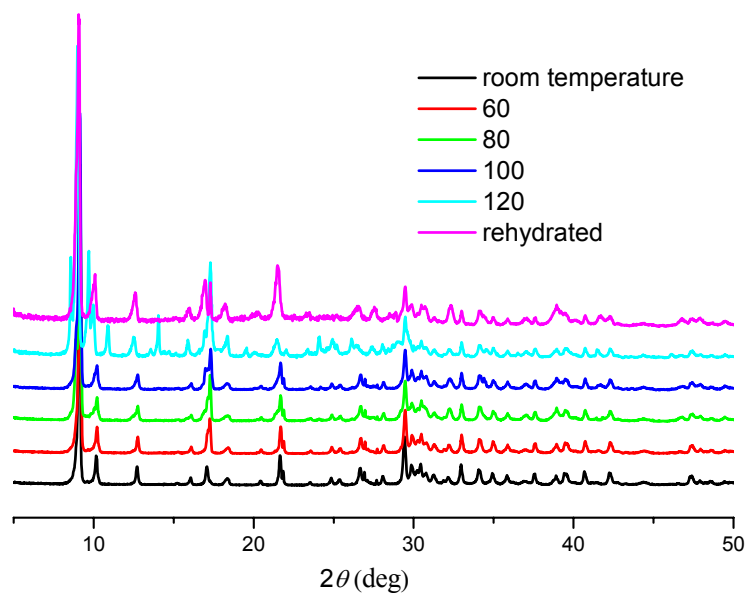


Fig. S10 PXRD patterns of **2** at different temperatures and the rehydrated product.

Table S1 Selective bond lengths (Å) and angles (°) for complexes **1** and **2***

1			
Ag(1)–O(1)	2.424(2)	Ag(1)–O(4)	2.446(2)
Ag(1)–O(2C)	2.667(3)	Ag(2)–O(1E)	2.559(3)
Ag(2)–O(2C)	2.361(2)	Ag(2)–O(3B)	2.250(2)
Ag(2)–O(4)	2.555(3)	Ag(2)–O(6D)	2.553(3)
Ag(1)⋯Ag(2)	3.327(1)	Ag(2)⋯Ag(2E)	2.943(1)
O(1)–Ag(1)–O(4)	95.75(8)	O(1)–Ag(1)–O(2C)	93.30(9)
O(2C)–Ag(1)–O(4)	82.63(8)	O(3B)–Ag(2)–O(2C)	161.02(8)
O(3B)–Ag(2)–O(6D)	116.76(8)	O(2C)–Ag(2)–O(6D)	82.13(8)
O(3B)–Ag(2)–O(4)	97.52(9)	O(2C)–Ag(2)–O(4)	86.76(9)
O(6D)–Ag(2)–O(4)	81.06(8)	O(3B)–Ag(2)–O(1E)	91.43(9)
O(2C)–Ag(2)–O(1E)	86.77(8)	O(6D)–Ag(2)–O(1E)	89.33(9)
O(4)–Ag(2)–O(1E)	169.07(8)		
2			
Ag(1)–O(1)	2.427(4)	Ag(1)–O(1C)	2.744(4)
Ag(1)–O(2B)	2.192(3)	Ag(1)–O(3A)	2.174(4)
Ag(1)⋯Ag(1D)	2.800(2)		
O(1)–Ag(1)–O(1C)	87.3(1)	O(1)–Ag(1)–O(2B)	106.2(1)
O(1)–Ag(1)–O(3A)	87.8(1)	O(1C)–Ag(1)–O(2B)	87.0(1)
O(1C)–Ag(1)–O(3A)	99.1(1)	O(2B)–Ag(1)–O(3A)	165.0(1)

* The symmetry codes are listed in Fig. S2 caption.